Jurnal Tribologi 46 (2025) 220-235

Jurnal Tribologi
Website : jurnaltribologi.mytribos.org
e-issn: 2289-7232

Friction and wear behavior of industrial waste reinforced anodic oxide coating under varying applied load

Norliyana Mustapar [1], Shahira Liza Kamis [1*], Kanao Fukuda [1], Noor Ayuma Mat Tahir [1], Yazid Yaakob [2], Intan Sharhida Othman [3]

[1] Malaysia-Japan International Institute of Technology, Universiti Teknologi Malaysia, MALAYSIA.
[2] Halal Product Research Institute, Universiti Putra Malaysia, MALAYSIA.
[3] Faculty of Industrial and Manufacturing Technology and Engineering, Universiti Teknikal Malaysia Melaka, MALAYSIA.
*Corresponding author: shahiraliza@utm.my

KEYWORDS

Hard anodizing
Industrial waste
Friction
Wear
Applied load

ABSTRACT

Hard anodizing produces a dense oxide layer but inherently consists of a porous structure that may compromise mechanical integrity. Incorporating ceramic reinforcements helps fill these pores, enhancing hardness, wear resistance, and overall durability. Nowadays, the use of industrial wastes as reinforcement alternatives can be considered a new technology in the field of material research for surface coating development. This work focuses on the friction and wear behavior investigation of anodic oxide coating without reinforcement (0 g/L), 100 g/L of industrial waste Fly ash reinforced anodic oxide coating (100 g/L IW_FA) and high purity commercial mullite reinforced anodic oxide coating (100 g/L HPC_M) under a wide range of applied loads (1 N-10 N). Results showed that as the applied load increases, the friction coefficient decreases (ranges from 0.54 to 0.43). Besides that, 100 g/L IW_FA showed the lowest wear rate (4.6×10^{-6} mm^3/Nm) even at high applied load (10 N) due to the formation of a transfer layer (oxide layer and FA) that attached to the counterpart. This beneficial behavior is mainly due to the potential properties of FA such as spherical particle shape, high hardness value and high specific heat capacity properties that enhanced tribological performance behavior at different applied load.

Received 11 March 2025; received in revised form 14 April 2025; accepted 25 June 2025.
To cite this article: Mustapar et al. (2025). Friction and wear behavior of industrial waste reinforced anodic oxide coating under varying applied load. Jurnal Tribologi 46, pp.220-235.

1.0 INTRODUCTION

Aluminum alloy surfaces can be enhanced through electrochemical anodization, which grows an oxide layer on the surface. This layer is known as the aluminum oxide coating. Aluminum oxide (Al_2O_3) coatings can be produced on aluminum alloys using a variety of electrolytes with direct current, or pulse current modes (Ding et al., 2018; Syamdri et al., 2020; Mohamad et al., 2020; Md. Ghazazi et al., 2023). Oxide layer can be categorizes based on their mechanical properties and the anodization process (Juhl et al., 2010). Anodizing is generally classified into three types. Type I anodization uses low current density chromic acid-based coatings with a thickness of around 1 μm (Khan et al., 2008). Type II anodization employs sulfuric acid-based coatings with higher current densities and thicknesses of 3-18 μm (Danford et al., 1992). While Type III anodization, also called hard anodizing, utilizes sulfuric acid-based coatings with high current densities and thicknesses exceeding 25 μm (Deng et al., 2004). It should be mentioned that anodic oxide layer consists of a barrier layer and porous layer, which both could affect the coating application greatly (Zhao et al., 2005; Tian et al., 2006). So, by filling the pores with reinforcement particles was attractive approach to enhance coating properties such as higher hardness and high wear resistance.

Over the years, great attention is paid on incorporating ceramic particles as reinforcement in anodic oxide coating. Examples of widely used ceramic particles include SiO_2, Al_2O_3, Mullite, SiC, TiO_2, and ZrO_2 (Li et al., 2014; Remešová et al., 2020). They demonstrate advantages in enhancing surface durability through increased surface hardness, improved wear properties, and corrosion resistance. A study by Nadimi et al. (Nadimi et al., 2022) discovered that the addition of SiO_2 particles to some extent improved the morphology of the coatings, which the porosity percentage of the coating was reduced by 30%. Incorporating SiO_2 as reinforcement on Al7075 also formed a dense coating, better microhardness, reduce friction and have anti-wear properties. In line with these findings, Zhang et al. (Zhang et al., 2013) results showed that Al_2O_3 particles can effectively increase wear resistance of composite oxide coating by embedded into the pores. The also found that friction coefficient reduction is mainly caused by the rolling effect of Al_2O_3 particles.

Our research group has explored the incorporation of industrial waste such as fly ash (FA), as a promising alternative solution, from both technological and economic perspectives, for improving mechanical properties and tribological performance (Mat Tahir et al., 2022; Mustapar et al., 2024). Fly ash, a byproduct of coal combustion in thermal power plants, poses significant environmental challenges (Selvam et al., 2013). Improper disposal of fly ash in landfills or ash ponds can lead to groundwater contamination due to the leaching of toxic elements (Sun et al., 2016). Utilizing FA, therefore, aligns with sustainability goals by repurposing industrial by-products, minimizing environmental impact, and providing a cost-effective solution for advanced surface engineering applications. Additionally, FA consist of multiple phases, which is quartz (SiO_2) and mullite ($3Al_2O_3{\cdot}2SiO_2$), whose benefits can be leveraged to enhance overall surface coating durability (Xing et al., 2019). The presence of quartz and mullite phase contributes to increased hardness and improves thermal stability of the coating, making FA a suitable reinforcement in anodic oxide coatings (Patil et al., 2020). By integrating these particles into oxide coatings, the resulting composite structures exhibit reduced surface roughness, improved load-bearing capacity, and lower wear rates under demanding contact conditions. Despite some efforts to utilize FA for various applications (Mahendra et al., 2010), in-depth studies on the ability of FA-reinforced anodic oxide coatings and their influence on tribological behavior under varying applied loads are limited. The aim of this paper is to fill this gap. Commercial mullite particles and anodic oxide coating without reinforcement were used for comparative research studies.

2.0 EXPERIMENTAL PROCEDURE

In this study, anodic oxide coatings were fabricated on AA2017-T4 alloy substrates using 20 wt% diluted sulphuric acid for anodizing process. The anodizing process was carried out at a constant current density of 15 A/dm^2 and fluctuating voltage of ±15 V. The reinforcement particles (industrial waste: FA and commercial particle: Mullite) were introduced into the electrolyte bath and stirred continuously to facilitate uniform coating formation. Three different coating variations were investigated: (i) anodic oxide coating without reinforcement (0 g/L), (ii) composite oxide coating incorporating industrial waste (100 g/L IW_FA) as a sustainable reinforcement material, and (iii) composite oxide coating reinforced with commercially available mullite (100 g/L HPC_M) for comparison. The compositions of 100 g/L for reinforcement particle were an optimal formulation based on our previous work (Mustapar et al., 2024). The mechanical properties of 0 g/L, 100 g/L IW_FA and 100 g/L HPC_M are shown in Table 1.

Table 1: Mechanical properties of 0 g/L, 100 g/L IW_FA and 100 g/L HPC_M (Mustapar et al., 2024)

Properties	**Anodic oxide coating**		
	0 g/L	**100 g/L IW_FA**	**100 g/L HPC_M**
Surface roughness (μm)	7.7	4.0	4.3
Surface hardness (Hv)	203.4	444.4	421.4

The friction and wear behaviors of all anodic oxide coating were evaluated using the ball-on-disc tribometer. The counterpart used was SUJ2 ball with a diameter of 8 mm. The schematic drawing of the test configuration is shown in Figure 1 and Table 2 shows the parameter used for the test. The sliding speed and sliding distance were fixed for all test conditions. During testing, the coefficient of friction (COF) was continuously recorded using a mechanical system throughout the sliding process. To ensure reliability, three measurements were taken from three separate samples under each test condition. The wear rate (k) was calculated using the Archard equation (Archard et al., 1953), as shown in Equation (1).

$$K = V/ FT \quad (1)$$

The overall wear volume, V, is determined by the applied normal load, F, and the total sliding distance, T, as expressed in the formula derived in the Equation (2) (Zulkifli et al., 2023).

$$V = AD \quad (2)$$

The cross-sectional area, A, was calculated using a 3D optical profiler, while the sliding diameter is represented by D. The worn surface morphology and chemical composition after the tribological tests were analyzed using SEM and EDS. Additionally, the wear volume of the tested samples was measured using a 3D optical profiler.

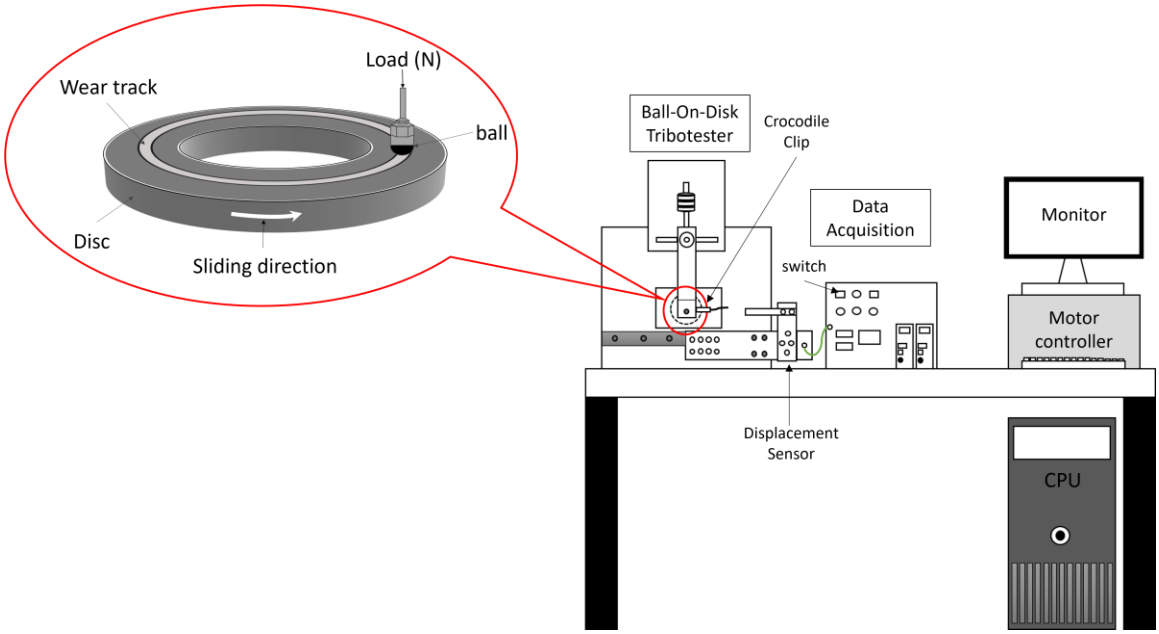

Figure 1: Schematic drawing of the ball-on-disc tribometer machine.

Table 2: Parameter applied on ball-on-disc tribometer machine.

Parameter	Details
Applied load (N)	1, 5, 10
Sliding speed (rpm)	30
Sliding distance (m)	1000

3.0 RESULTS AND DISCUSSION

Figure 2 and Figure 3 depict the friction coefficient curves of the anodic oxide coating (0 g/L), 100 g/L HPC_M and 100 g/L IW_FA under different applied loads. Both figures indicate that the friction coefficient decreases as the applied load on the ball-on-disc tribometer increases. When the applied load is 1 N, the friction coefficient is higher for all sample. The friction coefficient of coating (0 g/L), 100 g/L HPC_M and 100 g/L IW_FA are 0.54, 0.52 and 0.46, respectively. At 1N load (lower load), the contact pressure is relatively low, meaning that the real area of contact between the sliding surfaces also low. This limited real contact area with the small number of contact points leads to greater plowing resistance because the surface features are not yet fully flattened or compacted. These factors increase the friction coefficient at lower loads. While at 5N and 10 N load (higher load) was applied, the force applied to the surface is much greater, leading to higher contact pressure. This causes surface of anodic oxide coating deform and flatten, which could increase the real contact area and reduce localized stress. This is similar to previous study by Xu et al. (Xu et al., 2019) stated that the friction coefficient significantly decreases as the applied load increases due to the combined effects of compaction, tribo-layer formation and improved

load distribution. The formation of transfer layer acts as a lubricating agent to reduce direct surface interactions (Milan et al., 2005).

The composite oxide coating with reinforcement (100 g/L HPC_M and 100 g/L IW_FA) exhibited a lower friction coefficient compared to anodic oxide coating without reinforcement (0 g/L), indicating that the significant changes caused by the introduction of reinforcement into the oxide coating. The incorporation of reinforcement particles into the oxide coating fills the porous structure and enhances densification, which result in a smoother surface with lower roughness (as mentioned in Table 1). Smoother surfaces can improve load-bearing capacity by reducing asperity interactions, thereby reduce resistance to motion and lowering the friction coefficient (Fontaine et al., 2008; Sun et al., 2015). Other researchers also recorded similar behavior when incorporating reinforcement particles inside the oxide coating (Escobar et al., 2012; Atraszkiewicz et al., 2020; Muktar et al., 2024). Besides that, 100 g/L IW_FA exhibited the lowest friction coefficient and not significantly affected by different applied load, which is in accordance with its low surface roughness and spherical particle shape (Zhang et al., 2013). The spherical shape of fly ash (N. Niraj et al., 2018) allows a transition from sliding to rolling motion, significantly reducing friction coefficient. This occurs as the contact area with the surface decreases, effectively shifting from high sliding friction to much lower rolling friction. Essentially, only a tiny point of the sphere is in contact with the surface while rolling, resulting in less resistance to motion compared to when the entire flat surface is sliding across the ground (Myant et al., 2010; Lyashenko et al., 2022). In addition, 100 g/L IW_FA at 5 N (0.43) and 10 N (0.44) applied load did not make any significant changes on friction coefficient. This maybe due to saturation effect. After the reinforcement particles are sufficiently deformed or flattened under pressure as mentioned earlier, the actual contact area stabilizes, leading to similar friction coefficient values (as it evident in Figure 2 and Figure 3). Interestingly, as can be seen at the Figure 3, for 10 N applied load of all samples (0 g/L, 100 g/L HPC_M and 100 g/L IW_FA) was fluctuated in a very small extent value, which is 0.45, 0.44 and 0.44 respectively. This can be attributed to the nature of contact interaction between hard surfaces. The Al_2O_3 layer itself is a hard ceramic material, and the addition of hard ceramic reinforcement particles (FA and commercial Mullite) does not significantly alter the interfacial shear behavior under high load. This result was also supported by several researchers (Krishna et al., 2006; Zhang et al., 2013; Mohitfar et al., 2020), that reported at 10 N applied load, not much significant changes in friction coefficient for anodic oxide coating without reinforcement and anodic oxide coating with ceramic reinforcement. Moreover, it is worth to highlight that even different reinforcement type (current studies using FA and commercial mullite particles, while Zhang et al., 2013 using Al_2O_3 particles), as long as they are ceramic reinforcement particles, the fundamental interaction mechanism remains consistent, leading to similar friction behavior. Therefore, these findings indicate that the friction coefficient is strongly influenced by various factors as elaborated above.

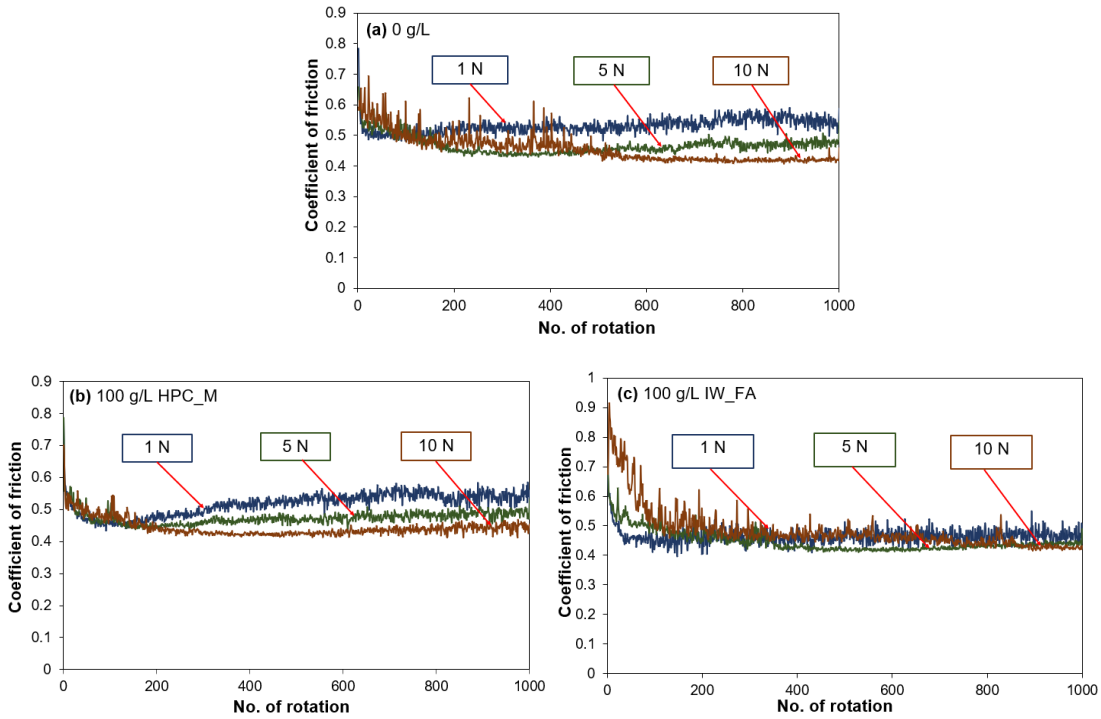

Figure 2: Friction coefficient curve for 0 g/L, 100 g/L HPC_M and 100 g/L IW_FA under different applied load.

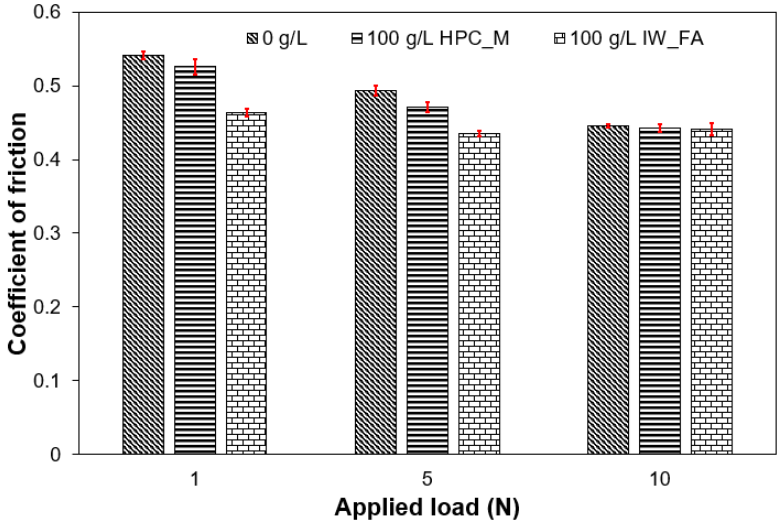

Figure 3: Average friction coefficient of 0 g/L, 100 g/L HPC_M and 100 g/L IW_FA under different applied load.

Figure 4 show the variation in wear rate of anodic oxide coating (0 g/L), 100 g/L HPC_M and 100 g/L IW_FA (was calculated according to Equation (1) and Equation (2)) at different applied

load, respectively. The results reveal a positive correlation between wear rate and applied load. The increase in wear rate with higher applied load can be attributed to the greater material deformation that occurs under increased stress. As the load is increase to 10 N, the contact pressure between the sliding surfaces rises, leading to accelerated plastic deformation within the composite oxide coating. This excessive deformation compromises the coating ability to effectively distribute the applied stress, reducing its load-bearing capacity and causing the coating to detach off easily. This detachment exposes the underlying surface to further wear, accelerating material loss and increasing the overall wear rate. This result was also discussed by (Odabas et al., 2018). Furthermore, several previous studies have reported that increasing the load often leads to deeper deformation layers on the wear surfaces (Chowdhury and Khalil et al., 2011; Z.Cheng et al., 2021).

As for the influence of incorporating reinforcement particles into the composite oxide coating (100 g/L HPC_M and 100 g/L IW_FA), the wear rate shows lower value compared to anodic oxide coating (0 g/L). The wear rate for composite oxide coating was in line with previous research that suggest the use of reinforcement materials with high hardness value, can not only increase hardness of the surface coating but also reduce the wear rate and increase service life of the material (Manohar et al., 2021; Khelge et al., 2022). The hardness of the composites oxide coating (100 g/L HPC_M and 100 g/L IW_FA) was evidently increased by the addition of commercial mullite and FA particles (as shown in Table 1), thereby reducing the wear rate value. Furthermore, previous literature has proven that incorporation of FA and commercial mullite particles increases hardness of the composite materials (Vinod et al., 2019; Roy et al., 2021). This is because FA and commercial mullite have the intrinsic properties of their constituent phases, primarily quartz and mullite. Quartz and mullite is known for its high hardness, making them more resistance to wear (Garcia et al., 2018; Mahnicka-Goremikina et al., 2022). This expected behavior also corroborated by Archard equation, Q = KWL/H, where Q is the wear volume, W is load, H is the hardness of material, K is a constant and L is the sliding distance. This relationship highlights that the increasing surface hardness of composite oxide coating, effectively reduces wear rate (Remešová et al., 2020). Additionally, as previously discussed, higher applied load increases the contact pressure, leading to higher frictional forces and consequently greater heat generation (Starostin et al., 2013; Kisuka et al., 2021). FA and commercial mullite consist of mullite structure, as mentioned earlier. Mullite has an excellent thermal characteristic, which is high specific heat capacity (around 4.22 J/g. K) (Roy et al., 2021). Hence, mullite can absorb and store more heat without a significant increase in temperature (Choo et al., 2019; Cao et al., 2024), this helps maintain temperature stability in environments where heat is generated, during frictional contact. In frictional contacts, reinforcement with high specific heat capacity properties help keep the surface temperature down, thus reduce wear rate (Ma et al., 2021). This result was also validated by specific heat capacity value in Figure 5.

A further decrease in wear rate was observed for 100 g/L IW_FA (4.6×10^{-6} mm^3/Nm) compared to 100 g/L HPC_M (5.4×10^{-6} mm^3/Nm) at 10 N. This result can be explained by electrophoretic effect phenomenon. In the anodizing, one of the mechanisms for incorporating reinforcement particles within the oxide coatings is through electrophoretic effects (Mu et al., 2012; Aziz et al., 2024). During anodizing process, the negatively charged reinforcement particles, are drawn toward the anode by the electric force. Based on previous studies have shown that FA possesses a negative surface charge of -23.08 mV (Mustapar et al., 2024). This strong electrostatic interaction between the FA (negative charge) and the anode (positively charge) leads to better bonding between the FA particles and the oxide coating, resulting in a surface with lower

roughness and higher hardness. In contrast, Commercial Mullite has a positive surface charge (40.86 mV). Therefore, FA particles migrate more towards the anode compared to Commercial Mullite and exhibit resistance to detachment during sliding, thus resulting in a lower wear rate. Further analysis will be done on the worn surface of 0 g/L, 100 g/L HPC_M and 100 g/L IW_FA.

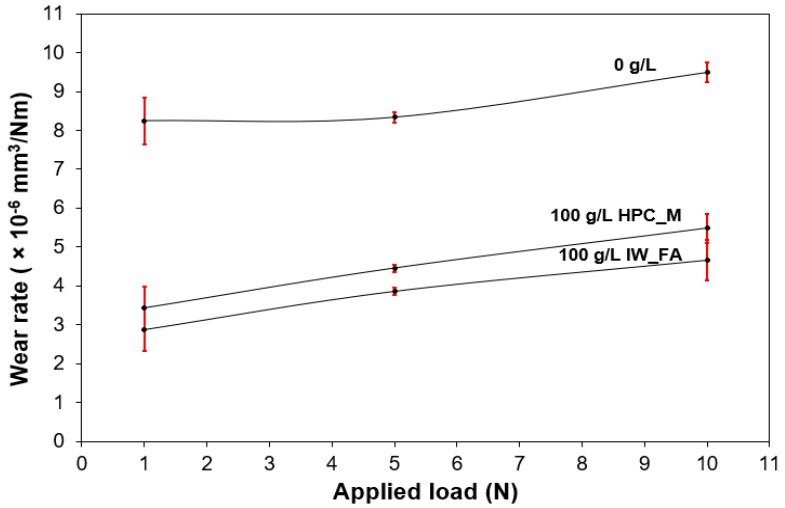

Figure 4: Variation in wear rate with different reinforcement particles at different applied load.

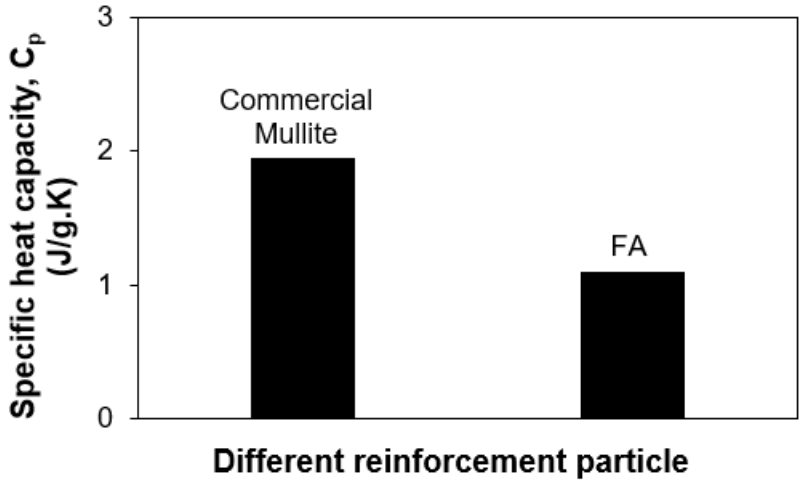

Figure 5: Variation in specific heat capacity of different reinforcement particle.

Effect of different applied load on the worn surfaces morphology of 0 g/L, 100 g/L HPC_M and 100 g/L IW_FA is shown in Figure 6. As can be seen from the SEM images, increasing applied load results in broader and more pronounced wear tracks. As the mechanical and thermal stress intensify under higher applied load conditions (Velugula et al., 2023), the composite oxide coating experiences increased material removal and leading to a wider wear scar on the surface of the disk. This observation highlights the direct influence of tribological parameters on the wear behavior of composite oxide coatings. The worn surface morphology of 0 g/L disk (Figure 6a) at

lower load (1 N) exhibits deep parallel grooves along sliding directions. There are many discontinuous oxide coating and accumulation of wear debris on the worn surfaces. These features indicate the dominant wear mechanisms of abrasive wear and plastic deformation. When the applied load is higher (5 N and 10 N), they are deeper grooves and ploughs, and almost no wear debris are present on the worn surfaces. Similar behavior has also been reported by Zeng et al. (Zeng et al., 2002), where the authors stated that the coating might totally worn off at higher load. Similarly for 100 g/L HPC_M and 100 g/L IW_FA worn surfaces, higher applied load exhibit larger wear track. However, the incorporation of reinforcement particles (commercial Mullite and FA) provides a significant contribution to tribological performance. This phenomenon is caused by the inclusion of reinforcement particles to the composite oxide coating creating higher surface hardness coating and acted as a lubricating agent during the sliding test (Nikoomanzari et al., 2020). Another factor that leads to lower wear and the oxide coating remained on the surface for 100 g/L IW_FA compared to 100 g/L HPC_M is the excellent thermal (high specific heat capacity) properties of FA, which effectively dissipate heat. It is known that during sliding, friction heat is produced, and composite oxide coating with good thermal properties can beneficially reduce wear (Dong et al., 2019).

In addition, as can be seen from (Figure 7) the wear scar of the SUJ2 counterpart for all samples, a greater amount of transfer layer formed on the ball surfaces when a higher load was applied. This indicates that the oxide layer transferred to the ball and covered the ball surface, hence helping to reduce the friction coefficient and wear as it may provide smooth sliding and act as protective interlayer for the counterpart against the composite oxide coating. For 100 g/L HPC_M and 100 g/L IW_FA, the reinforcement particles were also attached to the SUJ2 counterpart provide further decrease in wear. The presence of SiO_2 and Al_2O_3 element (as tabulated in Table 2) proved that transferred layers occurs during sliding. It is concluded that the worn surface morphologies under different applied loads in Figure 6 and Figure 7 can well interpret the wear rate evolutions in Figure 4. It is obvious that the wear mechanism at higher load (10 N) are typical abrasion and plastic deformations, which correspond to the high wear rate value.

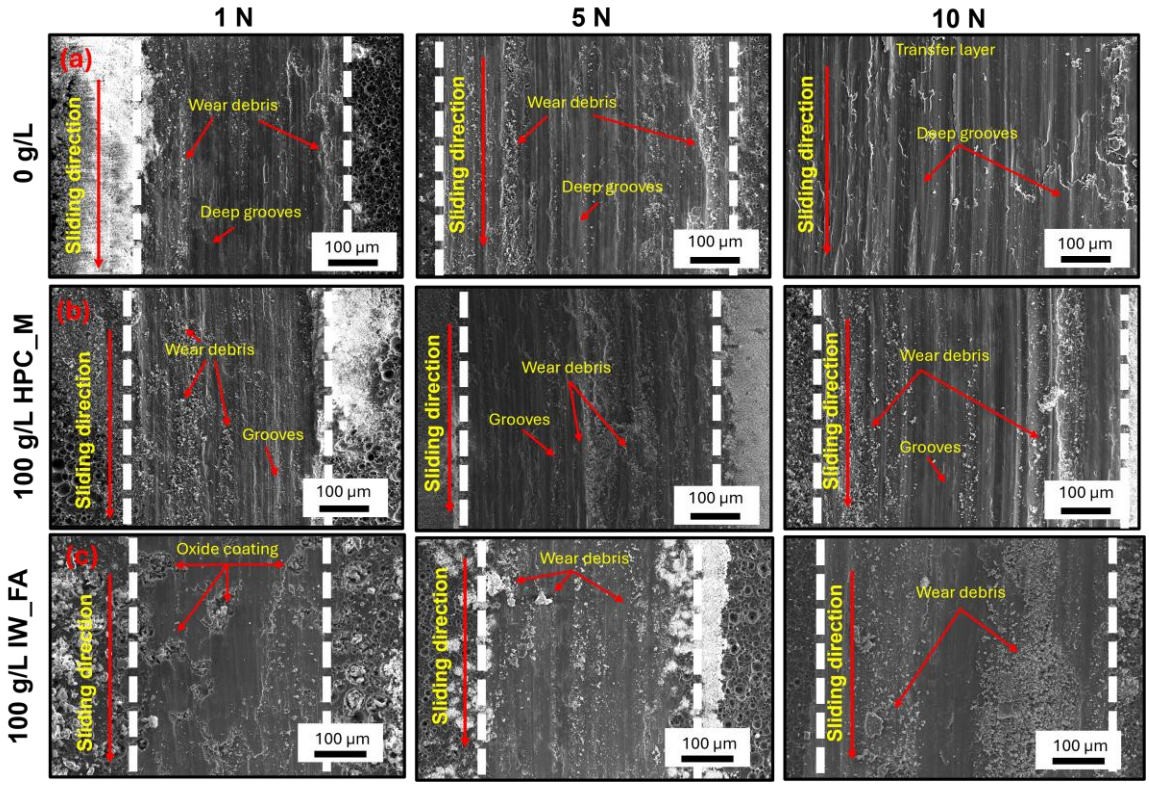

Figure 6: SEM image of (a) 0 g/L, (b) 100 g/L HPC_M, (c)100 g/L IW_FA wear track under different applied load.

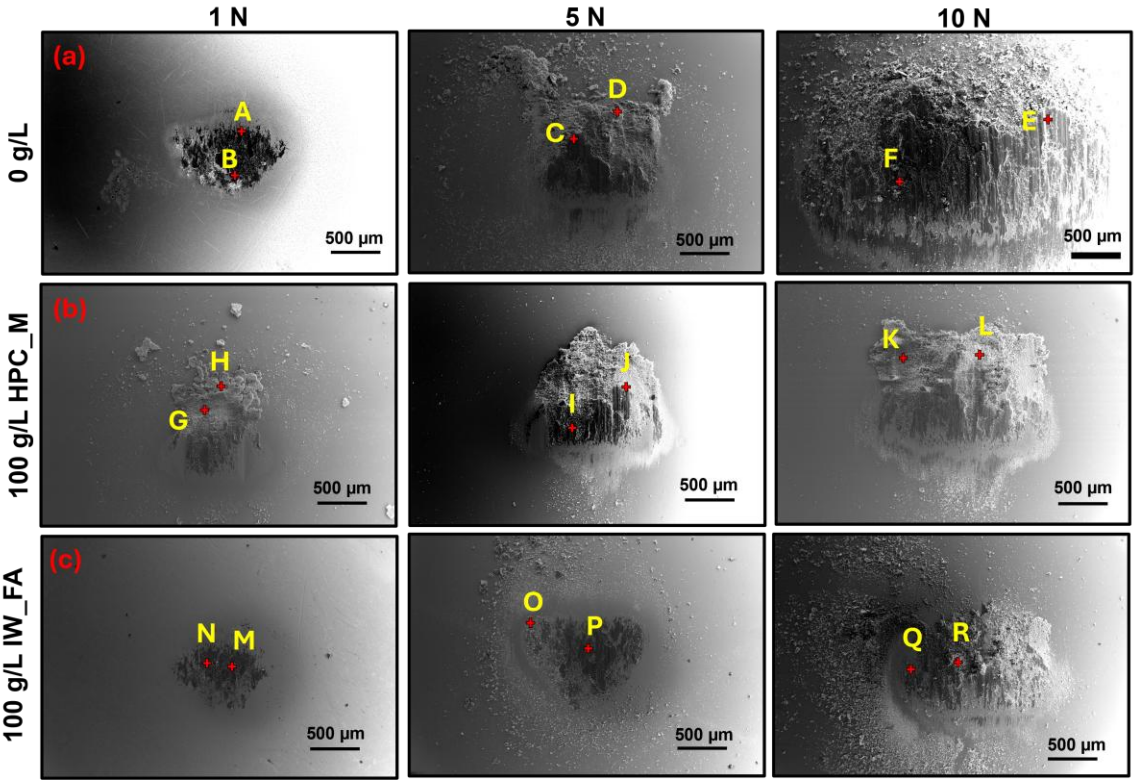

Figure 7: SEM image of (a) 0 g/L, (b) 100 g/L HPC_M, (c)100 g/L IW_FA wear scar ball under different applied load.

CONCLUSIONS

The findings of this study lead to the following conclusions:

(a) As the applied load increases, the friction coefficient decreases, this likely due to the increased contact pressure, which promotes surface deformation and compaction of the anodic oxide coating. This deformation leads to a smoother contact interface (flatten), increasing the real contact area while reducing localized stress concentrations. As a result, the sliding interaction becomes more stable, minimizing plowing effects and lowering overall friction coefficient.

(b) The addition of reinforcement particles, FA and commercial mullite improves friction coefficient and wear rate performance by filling the porosities, increasing densification, and creating a smoother surface. Additionally, FA with its spherical morphology enables a transition from sliding to rolling, further minimizing friction. Furthermore, the mullite phase (in the FA and commercial mullite) have a high specific heat capacity property, which absorbs heat and stabilizes surface temperature under high loads (10 N). This combined effect improves tribological performance and thermal stability of the surface coating.

(c) It should also be noted that the applied load for anodic oxide coating had a certain limit of 10 N. Above this optimal limit, there was no significant difference in friction coefficient.

The nature of contact interaction between hard surfaces accounts for this phenomenon. The Al_2O_3 layer is inherently a hard ceramic material, and the incorporation of hard ceramic reinforcement particles, including FA and commercial mullite, does not substantially alter the interfacial shear response under high load conditions. However, wear behavior still differs, as the 100 g/L IW_FA and 100 g/L HPC_M benefits from the load-bearing effect of the hard ceramics particles (FA and commercial mullite), which improve resistance to material removal, whereas the anodic oxide coating (0 g/L) experiences more severe wear due to its relatively lower hardness and weaker mechanical integrity.

Table 2: EDS analysis of wear scar of SUJ2 ball.

Spectrum	Weight (%)				
	Si	O	Al	C	Cu
A	-	47.70	47.81	2.04	2.45
B	-	48.88	43.84	4.94	2.35
C	-	42.89	52.60	1.44	3.08
D	-	38.34	57.32	1.93	2.42
E	-	17.74	75.88	1.81	4.57
F	-	27.15	66.46	2.36	4.03
G	-	37.61	58.61	1.83	1.95
H	0.89	46.66	47.94	2.28	2.22
I	-	46.13	48.90	2.21	2.76
J	0.40	40.18	55.72	1.33	2.37
K	0.67	38.31	57.61	1.32	2.09
L	-	38.21	57.55	1.66	2.58
M	0.35	32.28	61.16	2.48	3.74
N	0.37	49.54	44.04	3.30	2.75
O	1.77	36.57	52.20	6.58	2.87
P	0.55	29.44	60.86	5.20	3.94
Q	1.36	49.07	42.38	4.42	2.76
R	0.72	44.83	49.36	1.66	3.43

ACKNOWLEDGEMENT

The study is funding by the grant from the Ministry of Higher Education, Malaysia. Under Fundamental Research Grant Scheme (FRGS/1/2023/TK10/UTM/02/11).

REFERENCES

Archard, J. (1953). Contact and rubbing of flat surfaces. Journal of applied physics, 24(8), 981-988.

Atraszkiewicz, R., Makówka, M., Kołodziejczyk, Ł., Januszewicz, B., & Sucharkiewicz, J. (2020). Frictional behaviour of composite anodized layers on aluminium alloys. Materials, 13(17), 3747.

Aziz, A. A., Mamat, M. S., Kechik, M. M. A., Chan, K. F., Muktar, M. I., Tahir, N. A. M., ... & Yaakob, Y. (2024). Effect of anodizing voltage on surface and physical properties of CNTs incorporated aluminium oxide films. Jurnal Tribologi, 41, 144-161.

Cao, X., Zhao, K., Wang, L., Wang, T., Wu, Y., Tang, X., ... & Zhang, G. (2024). Robust, thermally insulating, and high-temperature resistant phosphate-enhanced mullite fiber porous ceramic composites. Ceramics International, 50(13), 23733-23743.

Cheng, Z., Yang, L., Huang, Z., Wan, T., Zhu, M., & Ren, F. (2021). Achieving low wear in a μ-phase reinforced high-entropy alloy and associated subsurface microstructure evolution. Wear, 474, 203755.

Choo, T. F., Mohd Salleh, M. A., Kok, K. Y., & Matori, K. A. (2019). A review on synthesis of mullite ceramics from industrial wastes. Recycling, 4(3), 39.

Chowdhury, M. A., Khalil, M. K., Nuruzzaman, D. M., & Rahaman, M. L. (2011). The effect of sliding speed and normal load on friction and wear property of aluminum. International Journal of Mechanical & Mechatronics Engineering, 11(1), 45-49.

Danford, M. D. (1992). A comparison of chromic acid and sulfuric acid anodizing (No. NASA-TM-108383).

Deng, P. Y., De Bai, X., Chen, X. W., & Feng, Q. L. (2004). Anodic oxidization of aluminum at high current densities and mechanism of film formation. Journal of The Electrochemical Society, 151(5), B284.

Ding, Z., Smith, B. A., Hebert, R. R., Zhang, W., & Jaworowski, M. R. (2018). Morphology perspective on chromic acid anodizing replacement by thin film sulfuric acid anodizing. Surface and Coatings Technology, 350, 31-39.

Dong, P., Long, C., Peng, Y., Peng, X., & Guo, F. (2019). Effect of coatings on thermal conductivity and tribological properties of aluminum foam/polyoxymethylene interpenetrating composites. Journal of Materials Science, 54(20), 13135-13146.

Escobar, J., Arurault, L., & Turq, V. (2012). Improvement of the tribological behavior of PTFE-anodic film composites prepared on 1050 aluminum substrate. Applied surface science, 258(20), 8199-8208.

Fontaine, J., Donnet, C., & Erdemir, A. (2008). Fundamentals of the tribology of DLC coatings. Tribology of Diamond-Like Carbon Films: Fundamentals and Applications, 139-154.

Garcia, D. C., Wang, K., & Figueiredo, R. B. (2018). The influences of quartz content and water-to-binder ratio on the microstructure and hardness of autoclaved Portland cement pastes. Cement and Concrete Composites, 91, 138-147.

Juhl, A. D. (2010). Overview of anodizing in the aerospace industry. Metal Finishing, 108(2), 20-21.

Khan, S. A., Miyashita, Y., Mutoh, Y., & Koike, T. (2008). Effect of anodized layer thickness on fatigue behavior of magnesium alloy. Materials Science and Engineering: A, 474(1-2), 261-269.

Khelge, S., Kumar, V., Shetty, V., & Kumaraswamy, J. (2022). Effect of reinforcement particles on the mechanical and wear properties of aluminium alloy composites. Materials Today: Proceedings, 52, 571-576.

Kisuka, F., Wu, C. Y., & Hare, C. (2021). Friction-induced heat generation between two particles. In EPJ Web of Conferences (Vol. 249, p. 05007). EDP Sciences.

Krishna, L. R., Purnima, A. S., & Sundararajan, G. (2006). A comparative study of tribological behavior of microarc oxidation and hard-anodized coatings. Wear, 261(10), 1095-1101.

Li, S., Zhu, M., Liu, J., Yu, M., Wu, L., Zhang, J., & Liang, H. (2014). Enhanced tribological behavior of anodic films containing SiC and PTFE nanoparticles on Ti6Al4V alloy. Applied surface science, 316, 28-35.

Lyashenko, I. A., & Popov, V. L. (2022). The influence of adhesion on rolling and sliding friction: An experiment. Technical Physics, 67(3), 203-214.

Ma, J., Wen, N., Wang, R., Wang, J., Zhang, X., Li, J., & Chen, Y. (2021). Effect of mullite film layers on the high-temperature oxidation resistance of AISI 304 stainless steel. Coatings, 11(8), 880.

Mahendra, K. V., & Radhakrishna, K. (2010). Characterization of stir cast Al—Cu—(fly ash+ SiC) hybrid metal matrix composites. Journal of Composite Materials, 44(8), 989-1005.

Mahnicka-Goremikina, L., Svinka, R., Svinka, V., Grase, L., Juhnevica, I., Rundans, M., ... & Fomenko, S. (2022). Thermal properties of porous mullite ceramics modified with microsized ZrO_2 and WO_3. Materials, 15(22), 7935.

Manohar, G., Pandey, K. M., & Maity, S. R. (2021). Characterization of Boron Carbide (B4C) particle reinforced aluminium metal matrix composites fabricated by powder metallurgy techniques–A review. Materials Today: Proceedings, 45, 6882-6888.

Mat Tahir, N. A., Liza, S., Fukuda, K., Mohamad, S., Hashimi, M. Z. F., Yunus, M. S. M., ... & Othman, I. S. (2022). Surface and tribological properties of oxide films on aluminium alloy through fly-ash reinforcement. Coatings, 12(2), 256.

Md. Ghazazi, N. A., Liza, S., Ishimatsu, J., Mat Tahir, N. A., Zulkifli, N. A., & Yaakob, Y. (2023). Effect of pulse current on surface properties of aluminum oxide coating containing graphite. Surface and Interface Analysis, 55(11), 831-844.

Milan, J. C. G., Carvalho, M. A., Xavier, R. R., Franco, S. D., & De Mello, J. D. B. (2005). Effect of temperature, normal load and pre-oxidation on the sliding wear of multi-component ferrous alloys. Wear, 259(1-6), 412-423.

Mohamad, S., Liza, S., & Yaakob, Y. (2020). Strengthening of the mechanical and tribological properties of composite oxide film formed on aluminum alloy with the addition of graphite. Surface and Coatings Technology, 403, 126435.

Mohitfar, S. H., Mahdavi, S., Etminanfar, M., & Khalil-Allafi, J. (2020). Characteristics and tribological behavior of the hard anodized 6061-T6 Al alloy. Journal of Alloys and Compounds, 842, 155988.

Mu, M., Zhou, X., Xiao, Q., Liang, J., & Huo, X. (2012). Preparation and tribological properties of self-lubricating TiO2/graphite composite coating on Ti6Al4V alloy. Applied Surface Science, 258(22), 8570-8576.

Muktar, M. I., Chan, K. F., Aziz, A. A., Zaid, M. H. M., & Shuhazlly, M. (2024). Surface characterization of oxide films formed on aluminium alloy with the incorporation of functionalized carbon nanotube. Jurnal Tribologi, 42, 85-102.

Mustapar, N., Liza, S., Fukuda, K., Tahir, N. A. M., Ishimatsu, J., Yaakob, Y., & Othman, I. S. (2024). Enhanced mechanical properties and tribological performance of anodic oxide coating by using thermal power plant waste material. Ceramics International, 50(20), 38372-38390.

Myant, C., Spikes, H. A., & Stokes, J. R. (2010). Influence of load and elastic properties on the rolling and sliding friction of lubricated compliant contacts. Tribology International, 43(1-2), 55-63.

Nadimi, M., Dehghanian, C., & Etemadmoghadam, A. (2022). Influence of SiO_2 nanoparticles incorporating into ceramic coatings generated by PEO on Aluminium alloy: Morphology, adhesion, corrosion, and wear resistance. Materials Today Communications, 31, 103587.

Nikoomanzari, E., Fattah-alhosseini, A., Alamoti, M. R. P., & Keshavarz, M. K. (2020). Effect of ZrO2 nanoparticles addition to PEO coatings on Ti–6Al–4V substrate: Microstructural analysis,

corrosion behavior and antibacterial effect of coatings in Hank's physiological solution. Ceramics International, 46(9), 13114-13124.

Niraj, N., Pandey, K. M., & Dey, A. (2018). Tribological behaviour of Magnesium Metal Matrix Composites reinforced with fly ash cenosphere. Materials Today: Proceedings, 5(9), 20138-20144.

Odabas, D. (2018). Effects of load and speed on wear rate of abrasive wear for 2014 Al alloy. In IOP conference series: materials science and engineering (Vol. 295, No. 1, p. 012008). IOP Publishing.

Patil, N. A., Pedapati, S. R., Mamat, O. B., & Hidayat Syah Lubis, A. M. (2020). Effect of SiC/fly ash reinforcement on surface properties of aluminum 7075 hybrid composites. Coatings, 10(6), 541.

Remešová, M., Tkachenko, S., Kvarda, D., Ročňáková, I., Gollas, B., Menelaou, M., ... & Kaiser, J. (2020). Effects of anodizing conditions and the addition of Al2O3/PTFE particles on the microstructure and the mechanical properties of porous anodic coatings on the AA1050 aluminium alloy. Applied Surface Science, 513, 145780.

Roy, R., Das, D., & Rout, P. K. (2021). A review of advanced mullite ceramics. Engineered Science, 18, 20-30.

Selvam, J. D. R., Smart, D. R., & Dinaharan, I. (2013). Microstructure and some mechanical properties of fly ash particulate reinforced AA6061 aluminum alloy composites prepared by compocasting. Materials & Design, 49, 28-34.

Starostin, N. P., Kondakov, A. S., & Vasilieva, M. A. (2013). Identification of friction heat generation in sliding bearing by temperature data. Inverse Problems in Science and Engineering, 21(2), 298-313.

Su, Y. S., Li, S. X., Gao, Q. Y., Jiang, H., Lu, S. Y., Yu, F., & Shu, X. D. (2019). Evolution of nano-laminated structure formed by the thermally assisted plastic deformation in dry sliding wear. Tribology International, 140, 105846.

Sun, W. C., Zhang, P., Zhao, K., Tian, M. M., & Wang, Y. (2015). Effect of graphite concentration on the friction and wear of Ni–Al2O3/graphite composite coatings by a combination of electrophoresis and electrodeposition. Wear, 342, 172-180.

Sun, X., Li, J., Zhao, X., Zhu, B., & Zhang, G. (2016). A review on the management of municipal solid waste fly ash in American. Procedia Environmental Sciences, 31, 535-540.

Syamdri, F. D., & Wibowo, R. (2020). The effect of sulphuric acid and oxalic acid on the formation of anodic aluminium oxide templates using two-step anodization method. In Journal of Physics: Conference Series (Vol. 1442, No. 1, p. 012063). IOP Publishing.

Tian, L. P., Zuo, Y., Zhao, X. H., Zhao, J. M., & Xiong, J. P. (2006). The improved corrosion resistance of anodic films on aluminum by nickel ions implantation. Surface and Coatings Technology, 201(6), 3246-3252.

Velugula, R., Thiruvallur loganathan, B., Varadhaiyengar, L., Asvathanarayanan, R., & Mittal, M. (2023). An Analysis of Mechanical and Thermal Stresses, Temperature and Displacement within the Transparent Cylinder and Piston Top of a Small Direct-Injection Spark-Ignition Optical Engine. Energies, 16(21), 7400.

Vinod, B., Ramanathan, S., Ananthi, V. et al. Fabrication and Characterization of Organic and In-Organic Reinforced A356 Aluminium Matrix Hybrid Composite by Improved Double-Stir Casting. Silicon 11, 817–829 (2019).

Xing, Y., Guo, F., Xu, M., Gui, X., Li, H., Li, G., ... & Han, H. (2019). Separation of unburned carbon from coal fly ash: A review. Powder Technology, 353, 372-384.

Xu, J., Chen, X., Grützmacher, P., Rosenkranz, A., Li, J., Jin, J., ... & Luo, J. (2019). Tribochemical behaviors of onion-like carbon films as high-performance solid lubricants with variable interfacial nanostructures. ACS Applied Materials & Interfaces, 11(28), 25535-25546.

Zeng, X. T., Zhang, S., Ding, X. Z., & Teer, D. G. (2002). Comparison of three types of carbon composite coatings with exceptional load-bearing capacity and high wear resistance. Thin Solid Films, 420, 366-370.

Zhang, D., Gou, Y., Liu, Y., & Guo, X. (2013). A composite anodizing coating containing superfine Al_2O_3 particles on AZ31 magnesium alloy. Surface and coatings Technology, 236, 52-57.

Zhao, Y., Chen, M., Zhang, Y., Xu, T., & Liu, W. (2005). A facile approach to formation of through-hole porous anodic aluminum oxide film. Materials Letters, 59(1), 40-43.

Zulkifli, N. A., Liza, S., Akasaka, H., Fukuda, K., Rawian, N. A. M., Ghazazi, N. A. M., ... & Yaakob, Y. (2023). Surface and tribology characterization of diamond-like carbon flakes reinforced oxide film by pulse anodizing. Ceramics International, 49(21), 34205-34222.